

## Polymer–Surfactant Layered Heterostructures by Electropolymerization of Phenosafranine in Langmuir–Blodgett Films

Shilpa N. Sawant,<sup>\*,†</sup> Mukesh Doble,<sup>‡</sup> J. V. Yakhmi,<sup>§</sup> S. K. Kulshreshtha,<sup>†</sup> Akira Miyazaki,<sup>||</sup> and Toshiaki Enoki<sup>||</sup>

Chemistry Division, BARC, Trombay 400085, India, Department of Biotechnology, Indian Institute of Technology, Chennai, India, Technical Physics & Prototype Engineering Division, BARC, Trombay 400085, India, and Department of Chemistry, Tokyo Institute of Technology, Ookayama, Meguro-ku, Tokyo, 152-8551, Japan

Received: June 8, 2006; In Final Form: August 25, 2006

Langmuir–Blodgett (LB) films of the water-soluble dye phenosafranine (PS) have been prepared by its adsorption from aqueous dye solution to an arachidic acid (AA) monolayer at the air–water interface. Atomic force microscopy (AFM) images of the LB films revealed the effect of change in pH of deposition on the degree of complexation of AA with the PS dye. Well-defined circular islands and holes were observed which disappeared with the increase in pH. Polarized absorption studies indicated that the dye molecules are oriented uniaxially with their long axis titled at a constant angle to the surface normal of the LB film. Within the restricted geometry of the LB film, the PS dye was electropolymerized to form a two-dimensional film of poly(phenosafranine) sandwiched between arachidic acid layers. The film was characterized by IR spectroscopy, cyclic voltammetry, and AFM. X-ray diffraction studies reveal the presence of a layer structure in the AA–PS LB film before and after polymerization. The polymer film showed highly anisotropic electrical conductivity of ca. 10 orders of magnitude. This indicates the formation of two-dimensional polyPS layers between arachidic acid layers resulting in a layered heterostructure film having alternate conducting and insulating regions. Also, the conductivity of the polyPS prepared from LB film was found to be  $\sim 2.5$  times higher than the conductivity of polyPS prepared by solution polymerization method.

### Introduction

Langmuir–Blodgett (LB) technique is widely used for the fabrication of films of a variety of advanced materials for application in molecular electronics,<sup>1</sup> biosensors,<sup>2</sup> and nonlinear optical (NLO) devices.<sup>3</sup> Conducting polymers are one such material that has attracted considerable interest in recent years. The preparation of high-quality ultrathin films of conducting polymers has great relevance to technological applications such as in sensors<sup>4</sup> and molecular electronics.<sup>5,6</sup> The poor solubility in common organic solvents and lack of amphiphilicity are two important factors that have restricted the LB deposition of conducting polymers. However, these factors have been overcome by various molecular engineering approaches. For example, solubility can be improved by attaching linear aliphatic side chains to the polymer backbone or by doping with an amphiphilic dopant.<sup>7–9</sup> Most often, the polymer is mixed with long chain matrix molecules for successful transfer to a substrate in order to obtain good LB films.<sup>10,11</sup> LB multilayer films of poly(*p*-phenylenevinylene) and poly(*p*-thiophenevinylene) have been prepared by depositing polyanion complexes of precursor polymers followed by polymerization of the multilayer film by exposure to heat.<sup>12,13</sup> Alternatively, direct use of surface-active monomer is also possible. The surface-active monomer can be polymerized either at the air–water interface<sup>14,15</sup> or after

deposition of LB films of the monomer on solid substrate.<sup>7,16</sup> As a strategy, if the monomer is arranged in the form of a well-ordered LB film and then polymerized, an ordered two-dimensional polymer can be obtained as against three-dimensional amorphous polymer films obtained with electropolymerization from solution. Manipulating the monomer structure or polymerizing monomers in highly organized or restricted media provides an opportunity to exercise control over the macroscopic properties of the polymer.<sup>16,17</sup> Hence polymerization of monomer in LB films or self-assembled monolayers (SAMs) is of importance. Bruno et al.<sup>18</sup> have reported enzyme-mediated synthesis of conjugated polymers at the air–water interface in a Langmuir trough. There are reports on the synthesis of conducting polymers using self-assembled monolayers of alkanethiols terminated by desired polymerizable tail groups.<sup>19</sup> Willicut et al.<sup>20,21</sup> have prepared SAMs of  $\omega$ -(*N*-pyrrolyl)alkanethiols, which were polymerized to obtain a two-dimensional film of polypyrrole. Onoda et al.<sup>22</sup> have reported a novel approach where, instead of manipulating monomers, trans oligomers were electropolymerized to prepare good-quality polythiophene derivatives.

Amphiphilicity of the film-forming material is a prerequisite for the formation of LB films. Therefore, in most of the reports, the monomer was covalently attached to the amphiphile, which hinders the mobility and limits the polymerization to a monolayer.<sup>15,23–25</sup> However, LB films of highly water-soluble functional molecules can also be fabricated without the requirement of synthesis of functional molecules containing long alkyl chains.<sup>26</sup> This involves the adsorption of water-soluble functional molecules (e.g., a dye) to amphiphilic molecules (e.g., arachidic

\* To whom correspondence should be addressed. Tel.: + 91-22 25590288. Fax: + 91-22 25505151. E-mail: stawde@barc.gov.in.

<sup>†</sup> Chemistry Division, BARC.

<sup>‡</sup> Indian Institute of Technology.

<sup>§</sup> Technical Physics & Prototype Engineering Division, BARC.

<sup>||</sup> Tokyo Institute of Technology.

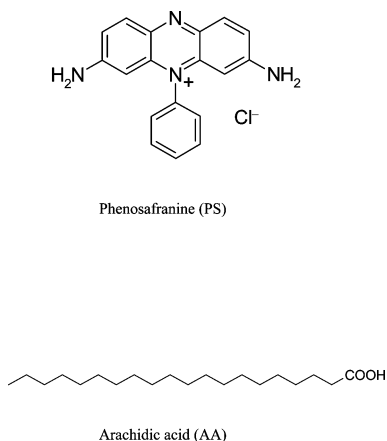


**Figure 1.** Structures of the materials employed in the preparation of LB films.

acid) at the air–water interface by either electrostatic interaction or hydrogen bonding. By choosing an appropriate amphiphile and parameters of deposition such as pH and deposition surface pressure, it is possible to tailor the orientation of the functional molecule to obtain the desired molecular arrangement.<sup>27</sup> As the electrostatic interaction between the oppositely charged adsorbate and adsorbent is a strong force, high adsorption can be obtained.<sup>28</sup> The advantage of electrostatic binding is that it does not “freeze” the orientation of the monomer but leaves it a sufficient degree of flexibility that is essential for electropolymerization.<sup>29</sup> Recently, Zhang et al.<sup>30</sup> have reported the polymerization of electrostatically bound aniline at the air–water interface. Rubner and co-workers,<sup>10,31,32</sup> have developed a novel method for deposition of LB film of conducting polymers using preformed polyion complexes of acid-functionalized conducting polymer and sterylamine. This approach is centered on the manipulation of surface-active polyion complexes formed by ionic binding of an amphiphile to the ionizable side groups of conjugated polymer. However, to our knowledge there are no reports on polymerization of electrostatically bound monomer in its multilayer LB film. In this paper, we describe a new method of fabricating LB films of conducting polymer by first forming LB film of the electrostatically bound monomer followed by its electropolymerization. The resulting LB film consists of monolayers of electroactive polymers isolated between insulating layers of amphiphilic molecules.

Phenazine and phenothiazine dyes, such as phenosafranin (3,7-diamino-5-phenylphenazinium chloride, Figure 1), are found to undergo electropolymerization<sup>33</sup> to yield a new class of electroactive polymers, commonly known as polyazines, which has attracted attention due to their good electron-mediating and electrocatalytic properties.<sup>34,35</sup> Poly(phenosafranin) modified electrodes have been reported to have excellent electrocatalytic activity for NADH ( $\beta$ -nicotinamide adenine dinucleotide) oxidation to enzymatically active NAD<sup>+</sup>. The NADH/NAD<sup>+</sup> redox couple is important because a large number of dehydrogenase enzymes use this coenzyme.<sup>36</sup> These electrodes are also used for detection of the neurotransmitter dopamine<sup>37</sup> in the presence of interfering ascorbic acid.<sup>38</sup> Hence, the formation of ordered and reproducible films of poly(phenosafranin) is important for its practical application in sensors.

In this paper, we report our studies on the fabrication of LB films of phenosafranin dye by adsorption of phenosafranin onto a monolayer of arachidic acid (eicosanoic acid) at the air–water interface. The film was transferred to conducting substrate and subjected to electrochemical polymerization to form poly-

(phenosafranin). The above strategy, in general, can be extended to the polymerization of technologically relevant conducting polymers in a multilayer LB film.

## Experimental Section

The molecular structures of arachidic acid (AA) and phenosafranin dye, employed in the preparation of LB films, is shown in Figure 1. Phenosafranin (Aldrich Chemical Co.) was purified by recrystallization from ethanol. Arachidic acid (Fluka Chemicals) was used without further purification. A KSV 5000 LB trough was used for studying the pressure–area ( $\pi$ - $A$ ) isotherms and for deposition of LB films. Surface pressure was measured with a platinum Wilhelmy plate. A compression rate of 5 mm/min was used for studying the pressure–area isotherm. Phenosafranin dye ( $1 \times 10^{-5}$  M) was used as the subphase, which was prepared from Millipore water (resistance > 18 M $\Omega$ cm), and its pH was adjusted using dilute NaOH or dilute HCl. The air–water interface was compressed and the surface layer was removed to remove any PS dye at the surface. The spreading solution was 1 mg/mL AA in chloroform (S. D. Fine Chemicals Ltd., India). After allowing 20 min for the chloroform to evaporate, the monolayer was compressed slowly to record the pressure–area isotherm. When the desired surface pressure was attained, the AA–PS complex monolayers were transferred from the air–water interface to solid substrate (glass or ITO) by the vertical dipping method. A surface pressure of 35 mN/m was maintained for deposition of LB films while the pH of the subphase was varied from 7 to 10. The dipping and raising speed was fixed at 5 mm/min, and a waiting time of 10 min was given between dips to dry the LB film. For optical absorption studies the film was deposited on quartz substrate and the absorption spectra were recorded on a Spectrascan UV-2600, India, double beam UV–vis spectrophotometer. LB films were deposited on CaF<sub>2</sub> crystal precoated with five layers of cadmium arachidate for IR studies. KBr pellets were prepared for polyPS synthesized by the LB route and by the solution polymerization method. IR spectra were recorded using a Jasco Model 610 FTIR spectrophotometer with a DTGS detector. X-ray diffraction (XRD) patterns were recorded on a Philips X-ray diffractometer (Model PW 1710) with Cu K $\alpha$  radiation ( $\lambda = 1.54056$  Å). The scan speed and step were 0.2 deg/min and 0.02 deg, respectively. Conductivity of the polymer film was measured by the two probe method. Circular gold contacts of 1 mm diameter were deposited on the film as well as on the adjacent bare ITO by the physical vapor deposition technique. Homemade micromanipulators were used to make contact, and the conductivity was measured using a Keithley electrometer. For measuring the in-plane or parallel conductivity of the film, any two contacts on the film surface were selected. The perpendicular conductivity was measured by selecting one contact on the LB film and other on the bare substrate where the film is not deposited. For conductivity calculation, the thickness of the polyPS LB film was derived from the bilayer separation obtained from XRD studies. In the case of polyPS film prepared by solution polymerization, the thickness was calculated based on the charge consumed during electropolymerization.

For atomic force microscopy (AFM) studies, three layered AA–PS LB films were deposited on mica substrate at different pH values of the subphase dye. ITO substrate was used for studying the morphology of polymer film before and after polymerization. AFM measurements were carried out using a scanning probe microscope (SPM-Solver P47, NT-MDT, Russia) in contact mode. Rectangular cantilevers of silicon nitride (length 200  $\mu$ m and width 40  $\mu$ m) having a force constant of 3

N/m were employed for the measurement. Particle size and roughness of the films were obtained using the software provided with the AFM. It calculates the average roughness ( $R_a$ ) using the formula

$$R_a = \frac{1}{N_x N_y} \sum_{i=1}^{N_x} \sum_{j=1}^{N_y} |Z(i,j) - Z_{\text{mean}}|$$

where  $Z$  is the  $Z$ -coordinate value and

$$Z_{\text{mean}} = \frac{1}{N_x N_y} \sum_{i=1}^{N_x} \sum_{j=1}^{N_y} Z(i,j)$$

Polymerization was carried out using a potentiostat–galvanostat PGSTAT20 (Eco Chemie, The Netherlands). A three-electrode system was used with platinum wire as the counter electrode and Ag/AgCl, 3 M KCl as the reference electrode. LB films deposited on ITO coated glass slides were electropolymerized in an aqueous acidic solution containing 0.05 M  $\text{H}_2\text{SO}_4$  under nitrogen atmosphere. For polymerization by potentiodynamic method, the voltage was scanned between  $-0.5$  and  $1.2$  V at a rate of  $50$  mV/s. Polymerization was also carried out using potentiostatic method by applying a voltage of  $1.3$  V for  $300$  s.

In order to estimate the size of AA–PS complex, molecular modeling studies<sup>39</sup> were carried out using the software HYPERCHEM version 7.0 (Hypercube Inc., USA). The structures of the dye, arachidate anion, and the anion–dye complex were optimized successively using the molecular force field method, MM+, semiempirical (PM3), and ab initio (minimal STO 3G basis set) methods to obtain the minimum energy conformation. The geometry minimization consists of starting the optimization from several initial starting geometries and letting the process converge to a minimum energy. The minimum of this set of minimum energies is assumed to be the global minimum energy, and the corresponding geometry is assumed to be the final geometry. The modeling calculations were carried out considering a constant dielectric medium corresponding to water.

## Results and Discussion

### Monolayer Characteristics at the Air–Water Interface.

The pressure–area ( $\pi$ – $A$ ) isotherms of arachidic acid (AA) spread on a subphase containing  $1 \times 10^{-5}$  M phenosafranin (PS) were measured at different pH values and compared with the corresponding isotherms in the absence of the dye in the subphase. Curve a in Figure 2 shows the pressure–area isotherm of AA on pure water (pH 5.8) at  $28^\circ\text{C}$ . The isotherm shows an abrupt increase in surface pressure at around  $25 \text{ \AA}^2$ . In the high-pressure region the curve is steep and shows a mean molecular area of  $22 \text{ \AA}^2$  (observed) corresponding to the true molecular cross section of arachidic acid.<sup>40</sup> The pH of the subphase was varied from 4 to 9.7 using HCl/NaOH, and the isotherms of AA in the absence of the dye were measured. It was found that the pressure–area isotherms remained essentially similar in the pH range 4–9.7 except for the presence of a plateau region at lower pressure in the case of pH 4. All the isotherms overlap well in the higher surface pressure region and give the same mean molecular area for the condensed phase. These observations are in accordance with the Gaines textbook<sup>40</sup> and the reports by Oishi et al.<sup>41</sup> where the pressure–area isotherms of AA monolayer were found to be identical in the pH range 3.3–9.6 at  $303$  K. Hence, only one representative plot (curve a)

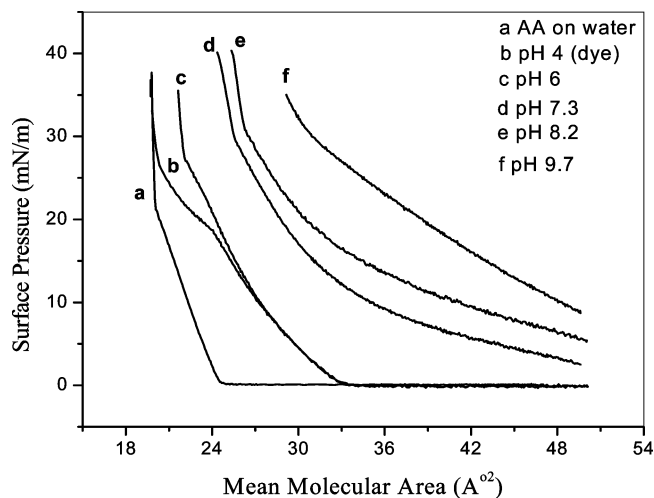


**Figure 2.** Pressure–area isotherms of arachidic acid on (a) water (pH 5.8) and (b–f) phenosafranin solution ( $1 \times 10^{-5}$  M) of pH 4, 6, 7.3, 8.2, and 9.7, respectively.

corresponding to AA monolayer on water in the absence of PS dye is shown in Figure 2.

The isotherm of AA on the aqueous solution of PS at pH 4 (Figure 2, curve b) exhibits an expanded isotherm at lower surface pressure compared to the isotherm of AA on pure water. This corresponds to compressible liquid phase<sup>42</sup> and indicates the presence of weak interaction (hydrogen bonding) between AA and PS. At higher surface pressures, the two isotherms overlap, giving similar mean molecular area (of  $22 \text{ \AA}^2$ ) and suggesting that there is no significant interaction between AA and PS in the solid phase at a subphase pH 4. As the pH of the dye solution is increased to 6 (Figure 2, curve c), an expanded isotherm corresponding to the compressible liquid phase is observed, which is similar to the isotherm at pH 4. However, at higher pressures the mean molecular area in the solid region increases to  $25 \text{ \AA}^2$ . This indicates the formation of a complex between AA and the dye and that the dye is adsorbed to the monolayer of AA at the air–water interface. At subphase pH values greater than 7, the isotherm is much more expanded at lower surface pressure and also shows a higher mean molecular area ( $>30 \text{ \AA}^2$ ) in the solid phase. Thus the amount of dye complexing to the AA layer was found to increase with increasing pH of the dye subphase. This is likely because, with increase in pH, the AA molecules ionize to produce anions, which attract the positively charged dye molecules to the surface. The  $pK_a$  of AA is 5.4,<sup>43</sup> which explains the change in the nature of isotherm (expansion of the isotherm) of the AA monolayer above pH 6, as observed in our experiments.

In order to confirm the presence of electrostatic interaction, IR spectra were recorded for AA–PS LB film, pure AA, and pure PS as shown in Figure 3. Sharp aliphatic CH stretching bands were observed at  $2915$  and  $2850 \text{ cm}^{-1}$  for both pure AA and AA–PS LB film. The carbonyl peaks at  $1685$  and  $1700 \text{ cm}^{-1}$  observed in the case of AA are absent in the case of AA–PS LB film. Instead, strong bands due to the asymmetric and symmetric stretching vibrations of the equivalent carbon–oxygen bonds are observed in the region  $1540$ – $1610 \text{ cm}^{-1}$  for the AA–PS LB film. This provides evidence for the presence of carboxylate anion in the LB film. Thus, in the AA–PS complex, the PS dye is electrostatically bound to the carboxylate group of AA. The packing of the dye molecules beneath the ionized AA monolayer is such that the mean molecular area of AA increases. However, considering the size of the PS dye molecule ( $\sim 11 \text{ \AA} \times 9 \text{ \AA} \times 4 \text{ \AA}$ , as obtained from modeling



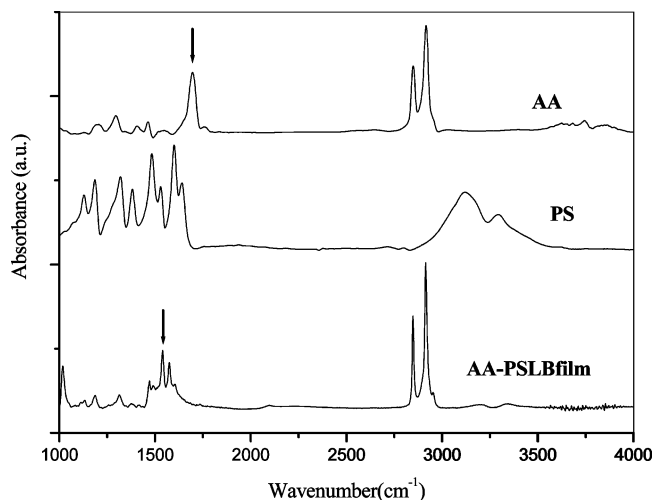


**Figure 3.** IR spectra of arachidic acid (AA), phenosafranine dye (PS), and AA-PS LB film deposited at a subphase pH 8.2.

studies), the observed increase in mean molecular area (MMA) is very small. This could be possible if the dye molecules remain adsorbed beneath the AA layer and there is not much penetration of the dye into the AA monolayer. Also, if not all the AA molecules are complexed with PS, i.e., there is incomplete complexation, the MMA increase will be small. There are several reports in the literature on adsorption of dyes to arachidic acid where the increase in MMA on adsorption of dye is very small compared to the dimensions of the dye. For example, the MMA of AA on cyanine blue solution was found by Saito et al.<sup>44</sup> to be  $31 \text{ \AA}^2$  at a surface pressure of 40 mN/m. Hada et al.<sup>45</sup> have reported a MMA shift of  $2 \text{ \AA}^2/\text{molecule}$  for adsorption of cyanine dye to AA. On the other hand, on adsorption of dyes to surfactants such as octadecylamine, a large increase in MMA is observed. Ray et al.<sup>46</sup> have reported a MMA shift of the order of the size of the dye molecule for the adsorption of sulforhodamine dye to octadecylamine. Similarly, Takahashi et al.<sup>27</sup> have observed a large change in MMA on adsorption of azo dyes to octadecylamine. In these cases, the dye molecules penetrate the surfactant layer, leading to a substantial increase in MMA.

The collapse pressure of AA monolayer was found to be around 65 mN/m when the pH of dye in the subphase was 8.25. The stability of the monolayer was inferred from the hysteresis of the  $\pi$ -A isotherm. For this, the monolayer was compressed to a fixed surface pressure value of 35 mN/m and subsequently relaxed to the original state. Very small hysteresis was observed during the first compression and decompression cycle for pH > 7. Later cycles were found to overlap well, indicating the formation of a stable monolayer at the air-water interface. Thus complexation with the PS dye gives stability to the AA monolayer as rendered on complexation with metal ions.<sup>42,47</sup>

**LB Film Formation.** The monolayers of AA-PS complex were transferred from the air-water interface to glass substrates at a surface pressure of 35 mN/m. Good LB films could be transferred onto substrates only above pH 7. The transfer ratio for upward and downward movements of substrate was found to be unity, indicating a Y-type deposition at pH > 7. At pH < 7, the transfer ratio was found to be negative for the downward movement of the substrate, which could be due to the desorption and/or dissolution of the deposited material. The nature of UV-vis absorption spectra of the films deposited in the pH range 7-10 was found to be essentially the same with peak maxima at 555 nm (plot 1 in Figure 4a). The LB film spectrum was found to be broader and is red-shifted compared with the

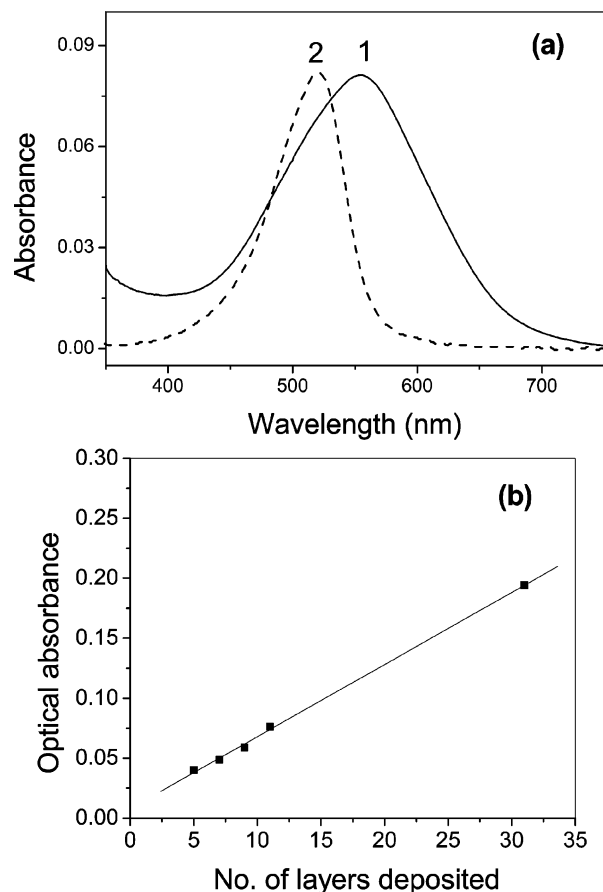


**Figure 4.** (a) UV-vis spectra of (1) AA-PS LB film and (2) aqueous solution of PS dye. (b) Optical absorbance vs number of monolayers deposited for AA-PS LB film deposited at a subphase pH 8.2.

solution spectra of PS<sup>48</sup> (plot 2 in Figure 4a). This broadening and large red shift in the absorption spectrum of the LB film can be attributed to the close packing ( $\pi$ - $\pi$  stacking) and aggregation of the dye molecules under the AA monolayer. The intensity of the absorption peak at 555 nm for the LB films deposited at each pH of the subphase was plotted against the number of monolayers transferred. Figure 4b shows one such representative plot for LB films transferred at a subphase pH 8.2. A linear plot was obtained for all depositions above a pH 7, indicating a regular and reproducible transfer of the AA-PS complex monolayer. For each pH of the dye in subphase, three films were deposited and the optical absorbance values were found to be highly reproducible ( $\pm 0.001$ ). Therefore, using this methodology, it is possible to control the amount of PS dye in the film precisely for any futuristic application.

**Orientation of the Dye in LB Film.** The orientation of the PS dye in the LB film of AA-PS was studied by polarized visible absorption spectroscopy.<sup>49</sup> Spectral anisotropy of a nine-layer LB film of AA-PS complex was studied by carrying out measurements with polarized light parallel (to the incident plane as p-wave) and perpendicular (s-wave) to the dipping direction as illustrated in Figure 5. The absorbance was recorded for incident polarized light falling at angles of  $0^\circ$  (normal incidence) and  $30^\circ$  to the normal of the film. Figure 6 shows plots for LB film deposited at subphase pH 8.2 (surface pressure = 35 mN/m). In the case of incidence angle of  $0^\circ$  (Figure 6a), no difference was observed in the absorption intensity for the s- and p-polarized lights, indicating that the transition moment of the PS dye is uniaxially distributed along the surface normal. In the case of the spectra recorded for polarized light incident at an angle of  $30^\circ$  (Figure 6b), the absorption intensity of the

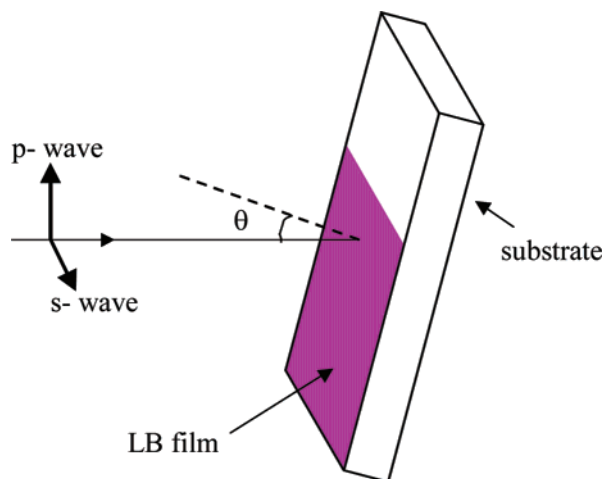


**Figure 5.** Schematic of experimental setup for polarized absorption studies.

s-wave was stronger than the intensity of p-wave. For unpolarized light, the spectra lies between the s- and p-polarized spectra. These results suggest that the PS molecules are arranged with their transition moments aligned at a constant angle to the surface normal of the LB film. A similar trend was observed for LB films deposited at other pH values; i.e., the absorption intensity of the s-wave was found to be stronger than the intensity of the p-wave. Ray et al.<sup>46</sup> have reported a similar tilted orientation of the transition moment of sulforhodamine dye adsorbed on octadecylamine LB films. A quantitative estimation of the tilt angle of the PS dye was made using the dichroic ratio of the absorbance at 555 nm. The LB film was assumed to be made of four phases where the refractive indices were assumed<sup>46,50</sup> to be  $n_1 = n_4 = 1.00$  (air),  $n_2 = 1.50$  (LB film), and  $n_3 = 1.54$  (substrate). Considering a uniaxial orientation of the transition dipole moment with the angle  $\theta$  with respect to the surface normal, the ratio between the p- and s-polarized absorption intensities is given by<sup>51</sup>

$$\frac{A_p}{A_s} = \frac{n_1 \cos i + n_3 \cos r}{n_1 \cos r + n_3 \cos i} \left[ \cos i \cos r + \frac{2n_1 n_3 \sin^2 i}{n_4 \tan^2 \theta} \right]$$

where  $i$  is the angle of incidence at the LB film and  $r$  is the angle of refraction at the LB film–substrate interface. The angle  $r$  can be calculated using the equation

$$n_1 \sin i = n_3 \sin r$$

From the above equations, a tilt angle of  $63^\circ$  was calculated for the PS molecule, which means that the long axis of the dye (i.e., line along the phenazine rings) is tilted at an angle of  $63^\circ$  to the surface normal. A tilted orientation of the PS dye molecule with respect to the arachidic acid chain (tilt angle  $\sim 60^\circ$ ) is also evident from the molecular modeling studies. The minimum energy conformation of the AA–PS complex is depicted in Figure 7. The dimensions of the complex were found to be  $0.997 \times 0.768 \times 3.026 \text{ nm}^3$ . Our aim was essentially to confirm that there is ordering of the dye molecules in the LB film before polymerization, which is clear from the polarized light absorption experiments.

**Surface Morphology Studies of AA–PS Film Using AFM.** AFM images were recorded for a three-layer LB film of AA–PS complex, deposited at different pH values of the subphase. The morphology of the AA–PS LB film deposited at subphase pH 7.5 is shown in Figure 8a. The film showed circular islands

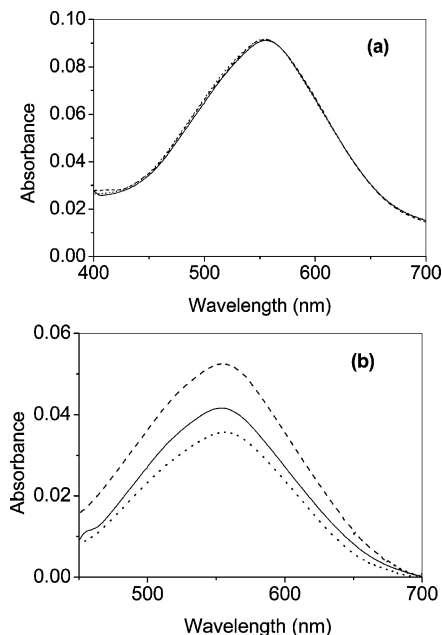


**Figure 6.** Polarized absorption spectra of nine-layer LB film of AA–PS complex at an incidence angle  $\theta$  of (a)  $0^\circ$  and (b)  $30^\circ$ . Dotted line: absorption spectra for p-polarized light. Dashed line: absorption spectra for s-polarized light. Solid line: absorption spectra for unpolarized light.

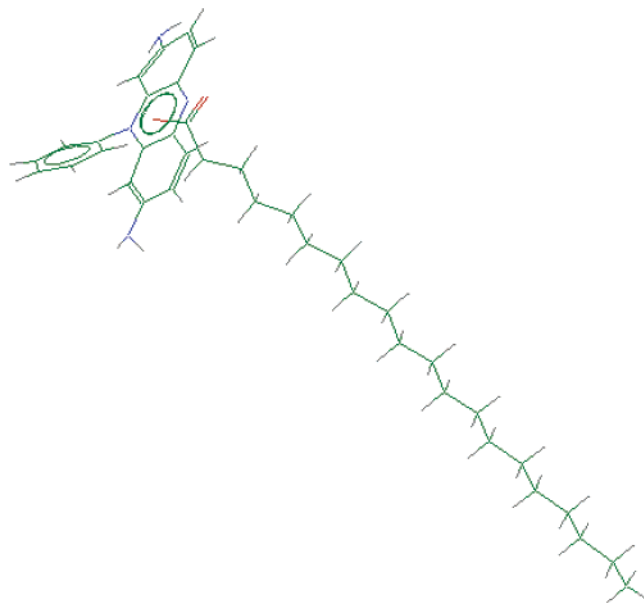


**Figure 7.** Structure of AA–PS complex obtained from ab initio quantum mechanical optimization using minimal STO3G basis set.

of height  $\sim 3.0\text{--}3.5 \text{ nm}$  and width  $\sim 200\text{--}800 \text{ nm}$  as shown in the cross-sectional profile along the line drawn in this figure. The minimum energy configuration for the AA–PS complex obtained from ab initio quantum mechanical optimization (Figure 7) corresponded to the dimensions  $0.997 \times 0.768 \times 3.026 \text{ nm}^3$ . Hence the height of the islands corresponds to the monolayer thickness. The island patches were found to arrange parallel to the substrate surface, hence maintaining the layer structure in the LB films. We believe that at this pH islands of ordered phase are formed due to incomplete complexation of AA with PS dye. Takahashi et al.<sup>52</sup> have reported formation of islands of  $\alpha$ -naphthol orange (NO) and methyl orange (MO) dyes on adsorption to LB film of octadecylamine.

The film deposited at higher subphase pH (pH 8.2) shows a smooth morphology with a number of circular holes (Figure

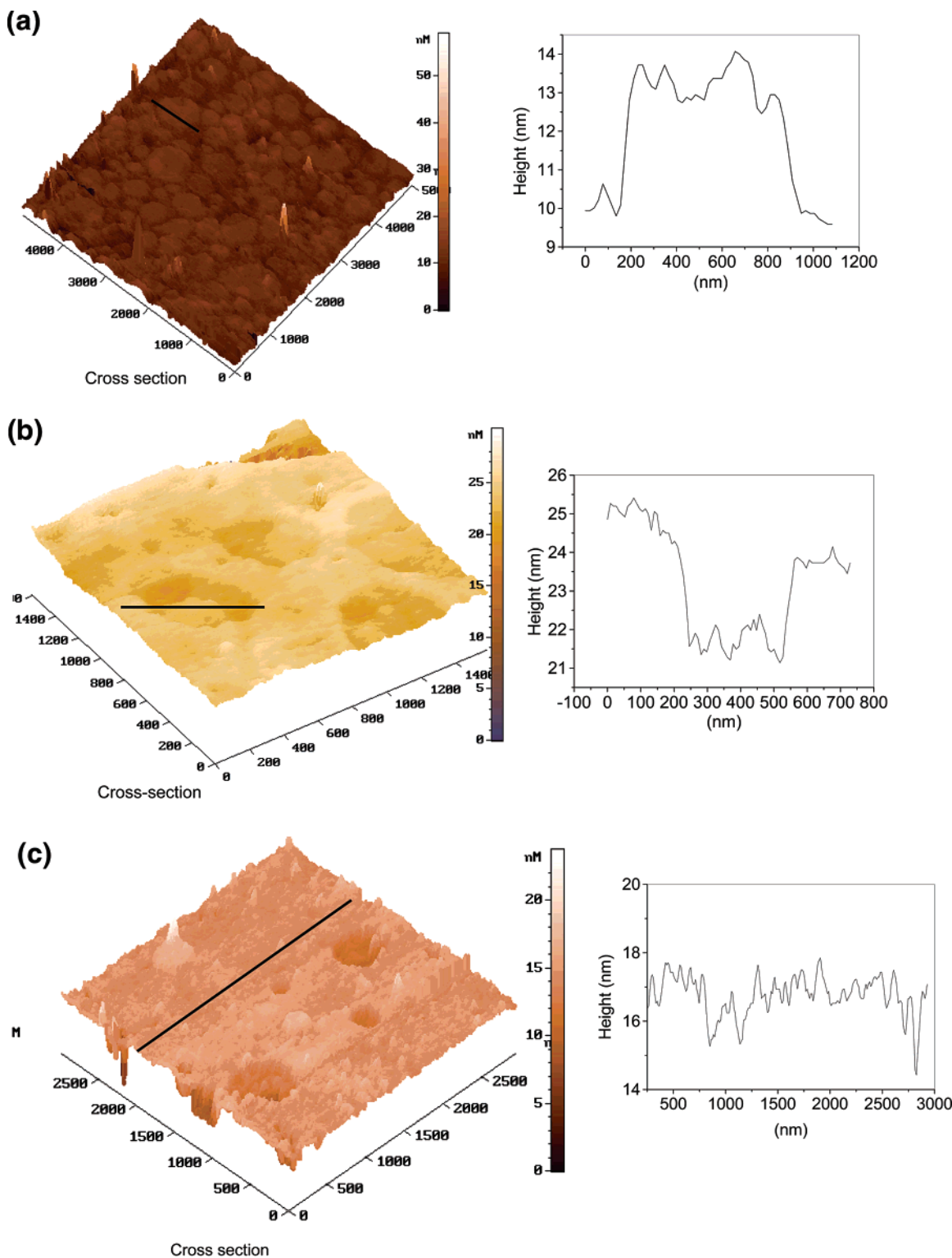


**Figure 8.** Surface morphology and cross-sectional view (along the line drawn) of LB film deposited at subphase dye pH (a) 7.5, (b) 8.2, and (c) 9.7, respectively.

8b). These holes have a depth of 3.0–3.5 nm and width of about 300 nm. The depth of the holes corresponds to the thickness of a monolayer. In this case the situation seems to be reversed, in the sense that now AA is complexed to PS in a much larger area leading to a smooth film with a few circular holes. These holes are much smaller in width compared to the circular islands observed at lower pH values of deposition. At still higher pH 9.7, a smooth film was obtained with just a few circular pits at some locations (Figure 8c). The density of holes was found to be less than that observed at pH 8.2.

The formation of LB films with circular holes having a depth of the order of the length of the amphiphile is reported in the literature.<sup>42,47</sup> During deposition of cadmium arachidate on mica at a pH 5.5, circular holes with 10–100 nm diameter were reported. However, upon increasing the pH, the number density of holes decreased and a uniform film was obtained at pH 6.5 as revealed from AFM measurements. Such pH-dependent changes in the morphology of the film of cadmium arachidate are consistent with the present observation on the AA–PS system. In both cases, the oppositely charged nature of PS or

$\text{Cd}^{2+}$  ions decreases the repulsion between the ionic groups within the monolayer by complexation with the AA. Thus oppositely charged counterions such as PS impart extra stability to the AA monolayer in way similar to that rendered by divalent metal ions. Moreover, such complexation can lead to efficient transfer of the monolayer to suitable substrates as revealed from the transfer ratio obtained during deposition.

**Electropolymerization of PS Dye.** The use of electrochemical polymerization for synthesis of conducting polymer LB films has been very limited despite the number of such polymeric films prepared so far: mostly chemical polymerization was used.<sup>5,53</sup> Electropolymerization of LB multilayers of amphiphilic pyrrole derivatives has been reported by Honda's group,<sup>16,54</sup> where they obtained anisotropic conducting film of polypyrrole having alternate conducting and insulating layers.

For electropolymerization of PS in the LB film, thick film with 31 layers of AA-PS complex were deposited on ITO coated glass slides. Both potentiodynamic and potentiostatic methods were attempted, and the results were compared with that of solution polymerization.

For solution polymerization, 0.5 mM PS in 0.05 M  $\text{H}_2\text{SO}_4$  was taken as electrolyte and the potential of the (bare) ITO electrode was scanned from  $-0.4$  to  $1.3$  V at the rate of  $50$  mV/s.<sup>38</sup> During the initial scans, phenosafranine shows an irreversible oxidation peak at  $1.2$  V corresponding to the oxidation of the amino ( $-\text{NH}_2$ ) group. As the scans progressed, a reversible peak starts to appear in the potential region  $0-0.1$  V. The height of this reversible peak increased successively, indicating the formation of the polymer, namely poly(phenosafranine), as shown in Figure 9a. These cyclic voltammograms (CVs) are in accordance with those reported in the literature for polymerization of PS dye from its aqueous solution.<sup>33,38</sup> The surface coverage of the electroactive sites in the film was estimated from the charge required to oxidize all the electroactive sites in the film, i.e., the charge under the oxidation peak in the CV of the film in  $0.05$  M  $\text{H}_2\text{SO}_4$ . The amount of electroactive species present at the electrode after 40 scans in the voltage range of  $-0.4$  to  $1.3$  V at the rate of  $50$  mV/s is  $1.8 \times 10^{-8}$  mol/cm<sup>2</sup>. Selvaraju et al.<sup>38</sup> have reported a surface coverage of  $7.4 \times 10^{-9}$  mol/cm<sup>2</sup> for deposition of polyPS in the scan range  $-0.5$  to  $1.3$  V at a scan rate of  $50$  mV/s for 25 cycles.

Polymerization of PS in the LB film was first attempted using potentiodynamic method, the details of which are mentioned in the Experimental Section. As the scans progressed, a reversible peak started appearing in the potential region  $-0.1$  to  $0.1$  V, which indicates the formation of poly(phenosafranine). Figure 9b shows 10 successive cyclic voltammograms recorded during the polymerization. As the scans progressed, the peak height decreased successively, contrary to that in the case of polymerization of PS from solution. The decrease is because the unpolymerized PS dye molecules, which are electrostatically bound, get desorbed and leach out of the LB film. The leaching out was also reflected by a change in the color of the electrolyte solution, which gradually turned purple-red. This is likely because in potentiodynamic method the polymerization occurs only for a fraction of time when the potential is above  $1.2$  V and hence the polymerization is slow compared to the leaching process. Moreover, electropolymerization of PS requires low-pH conditions at which AA in the LB film is expected to get protonated. This will lead to the release of the dye from the LB film. After about 50 scans, the CVs were found to saturate with no substantial reduction in peak height.

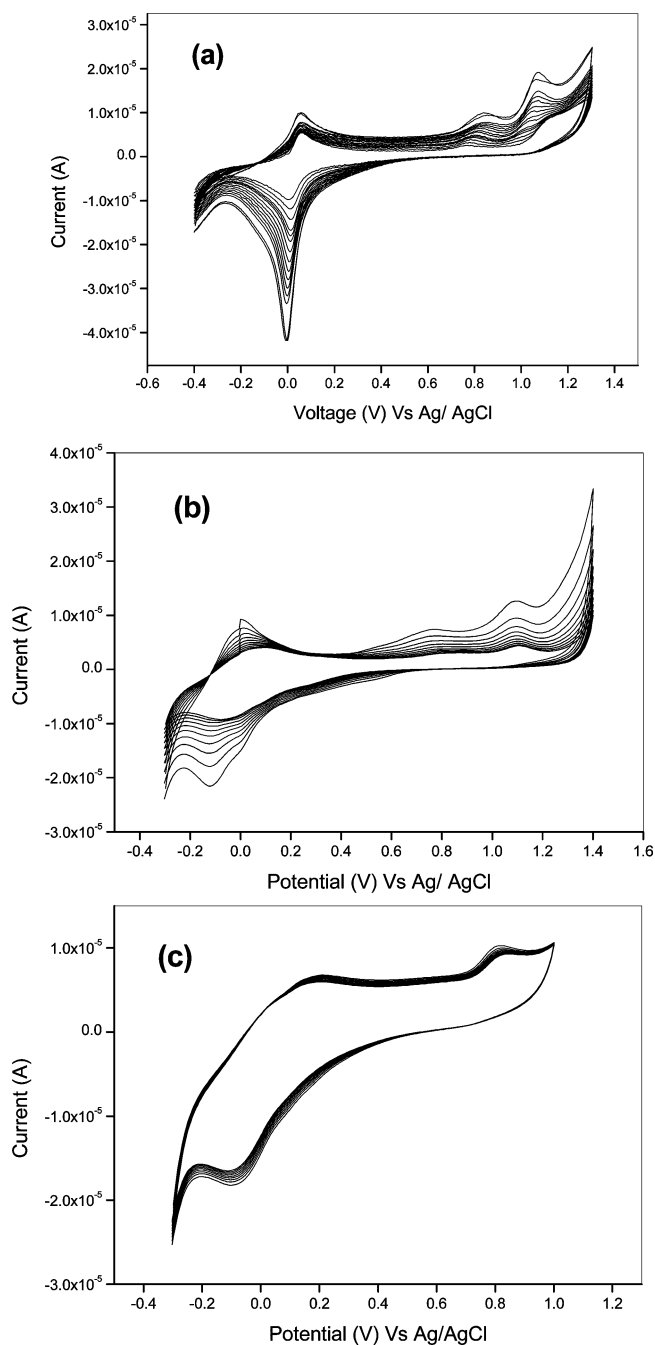


**Figure 9.** Cyclic voltammograms recorded (a) during solution polymerization of PS on bare ITO electrode, (b) during polymerization of PS in AA-PS LB film by potentiodynamic method, and (c) after polymerization of PS in the AA-PS LB film by potentiostatic method. Scan rate =  $50$  mV/s.

In view of the above-mentioned observations, potentiostatic method was adopted, which is expected to polymerize the electrostatically bound monomer quickly before it leaches out of the LB film. The voltage was applied as soon as the film was dipped in the electrolyte to avoid desorption of the dye. A purple-red water-insoluble film was obtained after polymerization. The electrolyte solution did not show much color change, indicating that there is no significant desorption of PS dye molecules from the LB film. After polymerization, cyclic voltammograms were recorded for the polymer film in  $0.05$  M  $\text{H}_2\text{SO}_4$  as depicted in Figure 9c. A reversible peak was observed in the voltage range  $-0.1$  to  $0.2$  V confirming the formation of poly(phenosafranine).



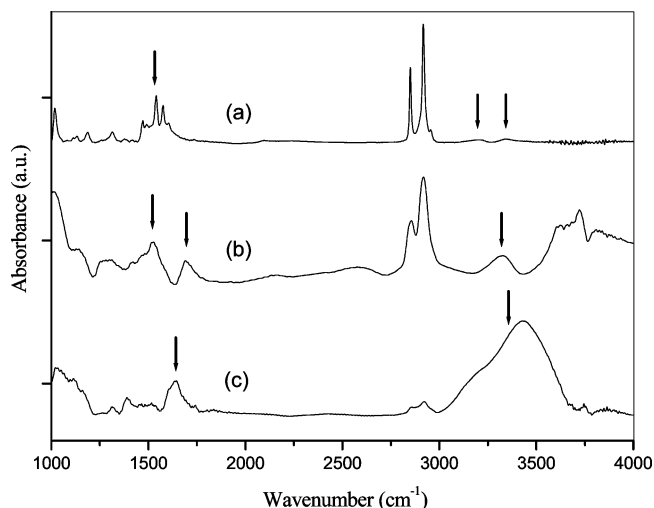


**Figure 10.** IR spectra of (a) AA-PS LB film, (b) polyPS prepared in LB film, and (c) polyPS prepared by solution polymerization respectively.

The peak height of the CV was found to decrease gradually in successive scans and reached saturation after about 25 scans. The reduction in peak height was much less compared to that observed in the case of polymer film obtained by potentiodynamic method and is likely to result from the leaching out of a small amount of monomer, which is not yet polymerized. The leaching out of monomer was found to be more pronounced for polymer film prepared at shorter polymerization time. Hence, the potentiostatic method was found to be the better method for polymerization of PS present in the LB film to form poly(phenosafranine). When the film was left dipped in water for more than 24 h, it developed cracks and peeled off from the ITO substrate to give small pieces of purple-red free-floating film.

From the charge consumed during electropolymerization, the number of electroactive PS species in the LB film was calculated to be  $5 \times 10^{-10}$  mol/cm<sup>2</sup>. This concentration of PS corresponds to a MMA of 33 Å<sup>2</sup>, which is higher than the MMA obtained from the pressure-area isotherm (29 Å<sup>2</sup>). The MMA obtained from the isotherm corresponds to the area occupied by the AA-PS complex. It will be the same as the MMA obtained from charge calculation if a 1:1 complexation is assumed. The charge calculation gives the actual number of PS molecules present in the film. Since the MMA or the area available to each PS molecule in the film (33 Å<sup>2</sup>) is higher than the area available to PS at the air-water interface, the number density of PS present in the film is less, suggesting that the degree of complexation is less than 1. AFM images of the films (Figure 8b) reveal the presence of a number of holes which could be due to incomplete complexation of AA as explained in the previous section.

**Structural Characterization of AA-PS LB Film before and after Polymerization of PS.** *IR Studies.* Figure 10 depicts the IR spectra of (a) AA-PS LB film, (b) polyPS prepared in LB film, and (c) polyPS prepared by solution polymerization, respectively. In the case of AA-PS LB film, two bands are observed at 3210 and 3350 cm<sup>-1</sup> with separation between them. These correspond to free asymmetric and symmetric stretching of the aromatic primary amine group of PS. On polymerization of PS, some of the primary amine groups couple with the aromatic ring of another PS molecule to form polymer, which will have secondary amine groups. For polyPS prepared in LB film (Figure 10b), a broad band is observed at 3325 cm<sup>-1</sup> corresponding to secondary amine group, thus confirming the

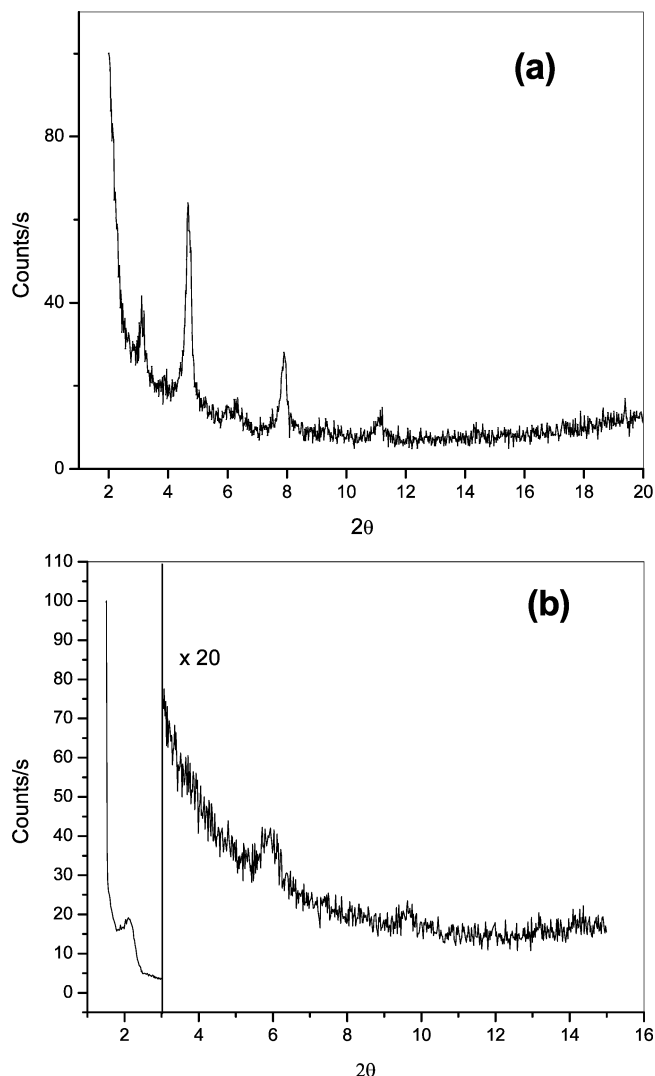


**Figure 11.** XRD patterns of a 31-layer AA-PS LB film (a) before and (b) after polymerization, respectively.

polymerization of PS to form polyPS. IR spectra of solution-polymerized PS (Figure 10c) also shows a broad band at 3430 cm<sup>-1</sup> corresponding to secondary amine group in the polymer. A band at 1640 cm<sup>-1</sup> is also observed which is attributed to NH bending mode in secondary amines. In the case of AA-PS LB film and polyPS prepared in LB film, the aliphatic CH stretch bands in the region 2800–2920 cm<sup>-1</sup> due to arachidic acid (AA) are very sharp and intense. Because of this, the amine bands appear to be relatively small compared to solution-polymerized PS where AA is absent. The band at 1540–1600 cm<sup>-1</sup> corresponding to carboxylate anion is present after polymerization of PS in the LB film (Figure 10b). In addition, the carbonyl peak at 1700 cm<sup>-1</sup> is also observed. This indicates that, on polymerization of PS in the AA-PS LB film, some of the arachidate ions get converted to arachidic acid.

*XRD Studies.* The periodic structure of the LB films was studied by X-ray diffraction measurement. Figure 11 shows the XRD patterns of a 31-layer AA-PS LB film (deposited on ITO glass at subphase pH 8.2) before (a) and after (b) polymerization. The profile of AA-PS LB film shows several sharp diffraction peaks corresponding to the (00*n*) planes, indicating the presence of a highly ordered layered structure. The bilayer spacing was found to be 5.638 nm, which is slightly less than twice the length, 3.026 nm, of the AA-PS complex. The length of AA acid itself is reported in the literature<sup>55</sup> to be 2.7 nm. Thus the



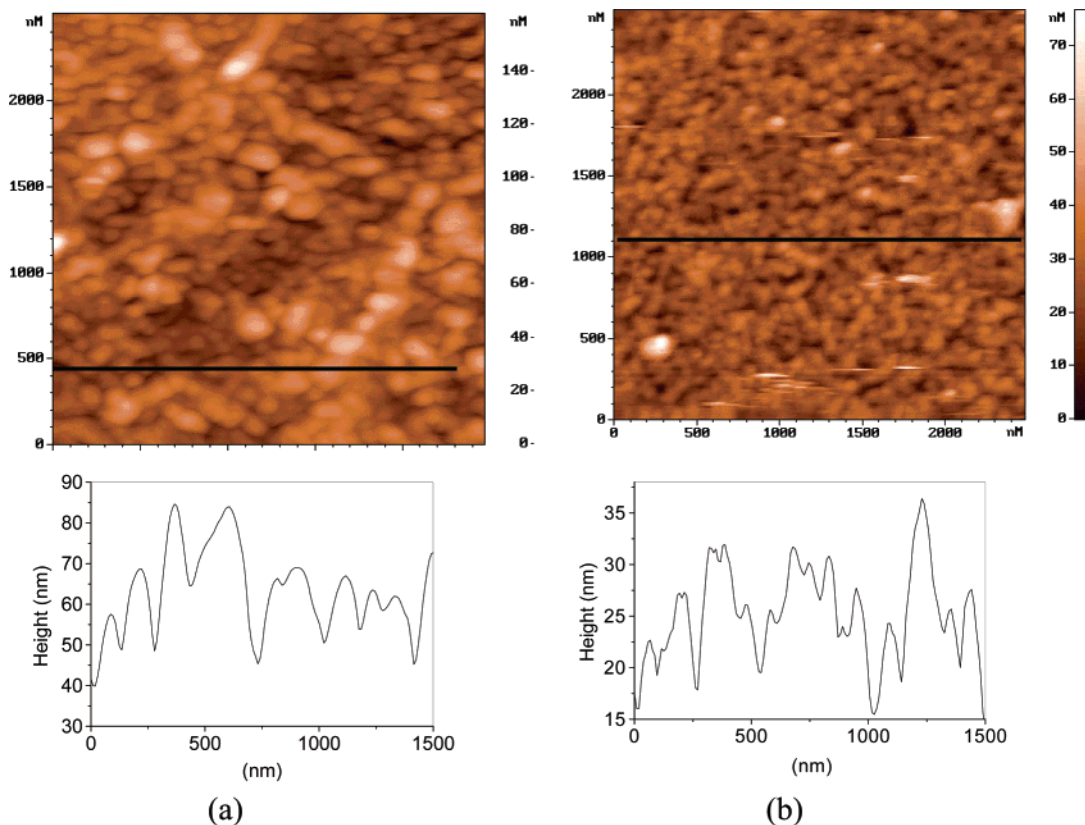


**Figure 12.** Surface morphology of 31-layer LB film of AA–PS complex (deposited on ITO substrate at subphase pH 8.2) (a) before and (b) after polymerization.

bilayer spacing obtained from XRD measurements is slightly less than twice the length of the AA–PS complex obtained from the modeling results. This can be explained by assuming an interdigitated structure where the hydrocarbon chain ends of the neighboring layers overlap each other<sup>27,28,46</sup> as well as have tilted orientation. Such an arrangement of the hydrocarbon chain can be expected in the case of dye adsorbed films because dye adsorption leads to an increase in the intermolecular distance as reflected from the increase in mean molecular area in the pressure–area isotherm (Figure 2). The increase in intermolecular distance results in a decrease in the lateral interaction between the hydrocarbon chains, which can be compensated in the case of interdigitated structure.<sup>27</sup> Thus the PS molecules fit in the void space between the hydrocarbon chains with the nitrogen of PS molecule in the vicinity of the carboxylic group of AA to facilitate ionic interaction.

On polymerization of the PS dye in the AA–PS LB film, the bilayer distance is reduced to 4.53 nm. The sharpness of the peaks is also reduced, but the layer structure remains intact. The further decrease of the bilayer thickness can be due to rearrangement of the AA and PS molecules in the LB film. The degree of interdigitation seems to further increase. The ionic bonding between PS and AA gives PS molecules the flexibility required to come close for polymerization to occur. Hence, on polymerization of the LB film, two-dimensional polymer layers are formed, which are separated by AA layers. This gives rise to a layered heterostructure having alternate polymer and AA layers as evidenced from XRD studies.

**AFM Studies.** Figure 12 shows the AFM images of 31-layer AA–PS complex (deposited on ITO substrate at pH 8.2) before (a) and after (b) polymerization. Before polymerization, granular features with an average width of 200 nm were observed. The whole scan area was selected to obtain the average surface roughness of the film. The average surface roughness was found

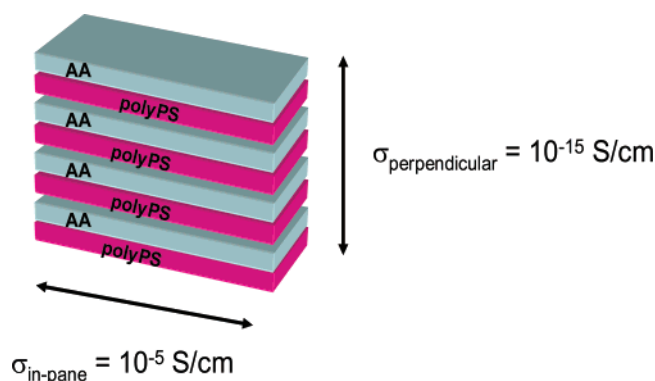


**Figure 13.** Anisotropic conductivity of polyPS LB film.

to be 15.7 nm. After polymerization, the grain size was found to reduce to an average of 50 nm. The surface roughness of the film is also reduced to 5 nm. Since the polymerization of PS dye in the layer structure occurs in a lateral fashion, it could probably lead to fragmentation of larger granular islands into finer regions, resulting in a uniform film.

**Conductivity Measurements.** The dc conductivity of the polymer LB film was measured using the two probe method. The conductivity was measured in two different geometries, namely, in-plane conductivity and conductivity across the film thickness (in the perpendicular direction), as shown in Figure 13. For a 31-layer polyPS LB film, the in-plane conductivity was found to be of the order of  $10^{-5}$  S/cm. The perpendicular conductivity, i.e., the conductivity across the film thickness, was found to be of the order of  $10^{-15}$  S/cm. Thus the polyPS LB film showed highly anisotropic dc conductivity of ca. 10 orders of magnitude. This highly anisotropic conductivity arises due to the presence of insulating AA layers in between the polymer layers in the LB film. Honda's group<sup>16,54</sup> have reported a similar

anisotropic conducting film prepared by polymerization of amphiphilic pyrrole derivative in its LB film. Their film had an alternating layered structure of a conducting polypyrrole layer and an insulating alkyl chain layer. The polypyrrole LB film showed a highly anisotropic dc conductivity of ca. 10 orders of magnitude.

The XRD and conductivity data provide evidence for the presence of a two-dimensional film of polyPS sandwiched between AA layers in the polyPS LB film. The conductivity of polyPS LB film prepared using the above method was found to be about 2–2.5 times higher than the conductivity of polyPS prepared by the solution polymerization method. Hence polymerization of PS molecules in the restricted geometry of its LB films helps in increasing the conductivity of polyPS.

Thus, two-dimensional multilayer films of poly(phenosafranin) could be prepared by restricting the monomer between arachidic acid monolayers in its LB film prior to its polymerization. The above strategy in general can be used for preparation of two-dimensional films of conducting polymers by first electrostatically binding the monomer to an oppositely charged amphiphile in an LB film and then carrying out its polymerization. Such a polymerization carried out in the restricted geometry of an LB film will help in increasing the conductivity of the conducting polymer thus formed. This method also allows generation of periodic heterostructures of ultrathin conducting and insulating layers which can be useful for application in nanotechnology-based devices.

## Conclusions

Phenosafranin, which does not contain any long alkyl chains, can be deposited as an LB film by its adsorption to arachidic acid monolayer. These monolayers could be successfully transferred from the air–water interface to obtain regular and reproducible LB films, as characterized by UV–vis absorption studies. Surface morphology of the films deposited at different pH values of the subphase, as studied by atomic force microscopy (AFM), showed circular islands and holes, which disappeared as the pH was increased to 9.7. Polarized visible absorption spectroscopy indicated that the dye molecules are oriented uniaxially with their transition dipoles aligned at an angle of 63° to the surface normal of the LB film. The ordered dye in the AA–PS complex LB film was electrochemically polymerized to form poly(phenosafranin). The resulting polymer LB film had a layered structure as indicated by the XRD measurements. The polyPS LB film showed higher in-plane conductivity compared to conductivity across the layer structure. These experiments indicate the presence of a two-dimensional film of polyPS sandwiched between AA layers in the polyPS LB film. Thus the resulting film consists of monolayers of electroactive polymer isolated by insulating layers of amphiphilic molecules. Also, the conductivity of the polyPS prepared by the LB route was found to be 2–2.5 times higher than the conductivity of polyPS prepared by the solution polymerization method. Hence the organization of the PS molecules in the LB film helped to increase the conductivity of polyPS.

The above strategy can be used for preparation of multilayer films of conducting polymers encapsulated by insulating layers. Since the thicknesses of the conducting and insulating layers are of the order of a few nanometers, this type of ultrathin heterostructure can be envisaged to help in the reduction of size of future molecular electronic devices.

**Acknowledgment.** We wish to thank Dr. P. A. Hassan, Dr. G. Ramakrishna, and Dr. Nitin Bagkar, BARC, for their kind

help and fruitful discussions. The authors also thank Dr. Mrinal Pai for IR measurements.

## References and Notes

- Albrecht, O.; Sakai, K.; Takimoto, K.; Matsuda, H.; Eguchi, K.; Nakagiri, T. *Molecular and Biomolecular Electronics*; Birge, R. R., Ed.; Advances in Chemistry Series 240; American Chemical Society: Washington, DC, 1994; p 341.
- Ihalainen, P.; Peltonen, J. *Langmuir* **2000**, *16*, 9571.
- Ashwell, G. J.; Dyer, A. N.; Green, A.; Sato, N.; Sakuma, T. *J. Mater. Chem.* **2000**, *10*, 2473.
- Potember, R.; Hoffman, R. C.; Hu, H. S.; Cocchiaro, J. E.; Viands, C. A.; Poehler, T. *Polymer* **1987**, *19*, 147.
- Conjugated Polymers*; Rubner, M. F., Skotheim, J. L., Bredas, J. L., Sibley, R., Eds.; Kluwer: Dordrecht, 1991; p 353.
- Handbook of Organic Conductive Molecules and Polymers*; Nakamura, T., Ed.; John Wiley & Sons, Inc.: New York, 1997; p 727.
- Ando, M.; Watanabe, Y.; Iyoda, T.; Honda, K.; Shimidzu, Y. *Thin Solid Films* **1989**, *179*, 225.
- Watanabe, I.; Hong, K.; Rubner, M. F. *Langmuir* **1990**, *6*, 1164.
- Riul, A.; Mattoso, L. H. C.; Mello, S. V.; Telles, G. D.; Oliveira, O. N. *Synth. Methods* **1995**, *71*, 2067.
- Cheung, J. H.; Rubner, M. F. *Thin Solid Films* **1994**, *244*, 990.
- Dhanabalan, A.; Dabke, R. B.; Datta, S. N.; Prasanth Kumar, N.; Major, S. S.; Talwar, S. S.; Contractor, A. Q. *Thin Solid Films* **1997**, *295*, 255.
- Era, M.; Kamiyama, K.; Yoshiura, K.; Momii, T.; Murata, H.; Tokito, S.; Tsutsui, T.; Saito, S. *Thin Solid Films* **1989**, *179*, 1.
- Nishikata, Y.; Kakimoto, M.; Imai, Y. *J. Chem. Soc., Chem. Commun.* **1988**, 1040.
- Hong, K.; Rosner, R. B.; Rubner, M. F. *Chem. Mater.* **1990**, *2*, 82.
- Kimkes, P.; Sohling, U.; Oostergetel, G. T.; Schouten, A. J. *Langmuir* **1996**, *12*, 3945.
- Shimidzu, T.; Iyoda, T.; Ando, M.; Ohtani, A.; Kaneko, T.; Honda, K. *Thin Solid Films* **1988**, *160*, 67.
- Watanabe, I.; Hong, K.; Rubner, M. F. *J. Chem. Soc., Chem. Commun.* **1989**, 123.
- Bruno, E. F.; Akkara, J. A.; Samuelson, L. A.; Kaplan, D. L.; Mandal, B. K.; Marx, K. A.; Kumar, J.; Tripathi, S. K. *Langmuir* **1995**, *11*, 889.
- Sayre, C. N.; Collard, D. M. *Langmuir* **1995**, *11*, 302.
- Willicut, R. J.; McCarley, R. L. *Adv. Mater.* **1995**, *7* (8), 759.
- Willicut, R. J.; McCarley, R. L. *Langmuir* **1995**, *11*, 296.
- Onoda, M.; Iwasa, T.; Kawai, T.; Nakayama, J.; Nakahara, H.; Yoshino, K. *J. Electrochem. Soc.* **1993**, *140*, 397.
- Kloppner, L. J.; Durna, R. S. *Langmuir* **1998**, *14*, 6734.
- Fichet, O.; Tran-Van, F.; Teyssie, D.; Chevrot, C. *Thin Solid Films* **2002**, *411*, 280.
- Hong, K.; Rubner, M. F. *Thin Solid Films* **1988**, *160*, 187.
- Engelsen, D. *J. Colloids Interface Sci.* **1973**, *45*, 1.
- Takahashi, M.; Kobayashi, K.; Takaoak, K.; Takada, Y.; Tajima, K. *Langmuir* **2000**, *16*, 6613.
- Ray, K.; Nakahara, H. *Bull. Chem. Soc. Jpn.* **2002**, *75*, 149392.
- Turyan, I.; Mandler, D. *J. Am. Chem. Soc.* **1998**, *120*, 10733.
- Zhang, J.; Mandler, D.; Unwin, P. R. *Chem. Commun.* **2004**, 450.
- Royappa, A. T.; Rubner, M. F. *Langmuir* **1992**, *8*, 3168.
- Cheung, J. H.; Punkka, E.; Rikukawa, M.; Rosner, R. B.; Royappa, A. T.; Rubner, M. F. *Thin Solid Films* **1992**, *210*, 246.
- Bauldrey, J. M.; Archer, M. D. *Electrochim. Acta* **1983**, *28* (11), 1515.
- Karyakin, A. A.; Karyakin, E. E.; Schmidt, H. L. *Electroanalysis* **1999**, *11*, 149.
- Inzelt, G.; Csahok, E. *Electroanalysis* **1999**, *11*, 744.
- Tanaka, K.; Tokuda, K.; Ohsaka, T. *J. Chem. Soc., Chem. Commun.* **1993**, 1770.
- Venton, B. J.; Wightman, R. M. *Anal. Chem.* **2003**, 414A.
- Selvaraju, T.; Ramraj, R. *Electrochem. Commun.* **2003**, *5*, 667.
- Leach, A. R. *Molecular modeling—principles and applications*, 2nd ed.; Prentice Hall: New York, 2001.
- Gaines, G. L. *Insoluble Monolayers at Liquid-Gas Interfaces*; Interscience: New York, 1966.
- Oishi, Y.; Takashima, Y.; Suehiro, K.; Kajiyama, T. *Langmuir* **1997**, *13*, 2527.
- Viswanathan, R.; Schwartz, D. K.; Garnes, J.; Zasadzinski, J. A. *Langmuir* **1992**, *8*, 1603.
- Bretts, J. J.; Pethica, B. A. *Trans. Faraday Soc.* **1956**, *52*, 1581.
- Saito, K.; Ikegami, K.; Kuroda, S.; Saito, M.; Tabe, Y.; Sugi, M. *J. Appl. Phys.* **1990**, *68* (5), 1968.
- Hada, H.; Hanawa, R.; Haraguchi, A.; Yonezawa, Y. *J. Phys. Chem.* **1985**, *89*, 560.
- Ray, K.; Nakahara, H. *J. Phys. Chem. B* **2002**, *106*, 92.
- Kurnaz, M. L.; Schwartz, D. K. *J. Phys. Chem.* **1996**, *100*, 11113.

(48) Arbeloa, I. L.; Rohatgi-Mukherjee, K. K. *Spectrochim. Acta, A* **1988**, 44 (4), 423.

(49) Akutsu, H.; Kyogoku, Y.; Nakahara, Y.; Fukuda, H. *Chem. Phys. Lipids* **1975**, 15, 222.

(50) Stanescu, M.; Samha, H.; Peristein, J.; Whitten, D. G. *Langmuir* **2000**, 16, 275.

(51) Vandevyer, M.; Barraud, A.; Texier, R.; Maillard, P.; Giannotti, C. *J. Colloid Interface Sci.* **1982**, 85, 571.

(52) Takahashi, M.; Kobayashi, K.; Takaoka, K.; Tajima, K. *Langmuir* **1997**, 13, 338.

(53) Goldenberg, L. M. *J. Electroanal. Chem.* **1994**, 379, 3.

(54) Iyoda, T.; Ando, M.; Kaneko, T.; Ohtani, A.; Shimidzu, T.; Honda, K. *Tetrahedron Lett.* **1986**, 27, 5633.

(55) Kondrashkina, E. A.; Hagedorn, K.; Vollhardt, D.; Schmidbauer, M.; Kohler, R. *Langmuir* **1996**, 12, 5148.